

# HPS2 - Demonstration of molten-salt in parabolic trough plants - Simulation results from system advisor model

Cite as: AIP Conference Proceedings **2303**, 110003 (2020); <https://doi.org/10.1063/5.0031276>  
 Published Online: 11 December 2020

Telma Lopes, Thomas Fasquelle, Hugo G. Silva, and Kai Schmitz



View Online



Export Citation



**Your Qubits. Measured.**  
 Meet the next generation of quantum analyzers

- Readout for up to 64 qubits
- Operation at up to 8.5 GHz, mixer-calibration-free
- Signal optimization with minimal latency

[Find out more](#)





# HPS2 - Demonstration of Molten-Salt in Parabolic Trough Plants - Simulation Results from System Advisor Model

Telma Lopes<sup>1</sup>, Thomas Fasquelle<sup>2</sup>, Hugo G. Silva<sup>3, a)</sup>, Kai Schmitz<sup>4</sup>

<sup>1</sup>*Renewable Energy Chair, University of Évora, Casa Cordovil, Rua D. Augusto Eduardo Nunes, n° 7, 7000-651 Évora, Portugal.*

<sup>2</sup>*IUSTI – Polytech Marseille Université d’Aix-Marseille, Marseille, France.*

<sup>3</sup>*Department of Physics and Earth Sciences Institute, School of Sciences and Technology, University of Évora, Rua Romão Ramalho, 59, 7000-671, Évora, Portugal.*

<sup>4</sup>*TSK Flagsol Engineering GmbH, Anna-Schneider-Steig 10, 50678 Cologne, Germany.*

<sup>a)</sup>Corresponding author: hgsilva@ueovra.pt

**Abstract.** High-Performance-Solar-2 (HPS2) is a parabolic trough demo project that is being built by a European consortium of research institutions (German Aerospace Center DLR, University of Évora) and companies (TSK-Flagsol, Rioglass, innogy SE, Steinmüller Engineering, Yara, eltherm) on the Evora Molten Salt Platform (EMSP). The purpose of this plant is to demonstrate the viability of using molten salts as heat transfer fluid in parabolic trough power plants, while performing research and development on such technology. Commissioning of the power plant is foreseen for the end of 2020. Meanwhile, a theoretical study consisting of an annual simulation with NREL’s System Advisor Model (SAM) has been performed to support consolidate the test plan of the platform with possible operation strategies to avoid freezing of the salts.

## INTRODUCTION

HPS2 features a solar field of parabolic trough collectors with a total length of 684 m and an aperture of 6.77 m designed to attain ~3.6 MW<sub>th</sub> nominal power. High temperatures can be reached thanks to a concentration factor of ~31 (considering the absorber tube’s external surface as receiving area) or ~97 (considering the product of the diameter and the length of the absorber tube as receiving area) and PTR<sup>®</sup>70-5G Advanced Receivers. The temperature range will be 290 °C – 500 °C. Heat transfer fluid (HTF), YARA-MOST, consists of a ternary mixture based on potassium nitrate (KNO<sub>3</sub>), sodium nitrate (NaNO<sub>3</sub>) and as source of calcium nitrate Yara NitCal-K, a patented double salt KNO<sub>3</sub>.5Ca(NO<sub>3</sub>)<sub>2</sub>.10H<sub>2</sub>O; with a proportion of 43% KNO<sub>3</sub>, 15% NaNO<sub>3</sub> and 42% Ca(NO<sub>3</sub>)<sub>2</sub>. This ternary mixture has a similar composition as the Hitec XL salt and has a melting point of 131 °C. Maximum operating temperature is foreseen to be at least 500 °C and will be studied during this experimental project. The test plant is also composed of a two-tank (H = 5 m, D = 3.1 m, H<sub>eff</sub> = 3.1 m) thermal energy storage (TES) system with a theoretical capacity of 4.4 MWh. A complete Steam Generator System (SGS) absorbs up to 1.8 MW<sub>th</sub> of the produced heat in order to produce 140 bar and 500 °C superheated steam; parameters that allow for an efficient conversion of heat to electricity in commercial plant arrangements through a steam turbine. Within HPS2, no turbine will be installed and thus the superheated steam is condensed through dry-cooling and sent back to the feedwater tank [1].

## HPS2 THERMAL STUDY

Since the use of molten salts as heat transfer fluid (HTF) allows to increase the operating temperature of such plants, the thermal losses that occur there will also increase. In order to assess this variation, this section will determine the thermal losses on interconnecting piping and receiver tubes during nominal operation of the platform. In addition,

the thermal losses during night and thermal inertia capacity of the cold tank will be determined in order to define operating strategies.

### Thermal Losses in the Piping

Thermal losses are calculated for the piping zones appearing on **FIGURE 1**. Zone 1 (at 500 °C) and 4 (at 290 °C) are the interconnecting piping between the solar field and the tanks; zone 2 (at 500 °C) and 3 (at 290 °C) connect the tanks to the steam generator system; zone 5 (at ~400 °C) is the crossover piping between the two lines of collectors. Calculations were made for each zone, according to their characteristics (HTF temperature and length).

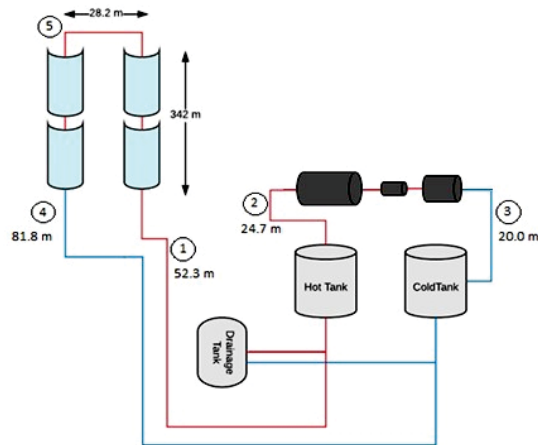


**FIGURE 1.** Diagram of the plant with the 5 different pipe zones marked. Hot lines appear in red and cold lines in blue.

It is assumed that all pipes have the same diameter of 3” (although about 5 % of the plant is composed of 2” pipes where equipment, such as valves, are located) and a rockwool insulation thickness of 15 cm. In order to calculate thermal losses in the piping, three processes must be considered:

1. convective heat exchange between HTF and the piping (represented by a convective resistance,  $R_{conv}^{f-p}$ )
2. conduction through the piping insulation (represented by a conduction resistance,  $R_{cond}^i$ )
3. convective heat exchange between the outer piping insulation and the air (represented by a convective resistance,  $R_{conv}^{i-a}$ ).

Radiative losses depend on the surface emissivity, the system temperature and the temperature difference between the surface and the environment. As ambient and surface temperatures are very close and the piping is protected by a low emissivity aluminium surface [2], the radiative losses can be neglected. Conduction resistance through this surface is also neglected because its thickness is very small and its thermal conductivity is very high.

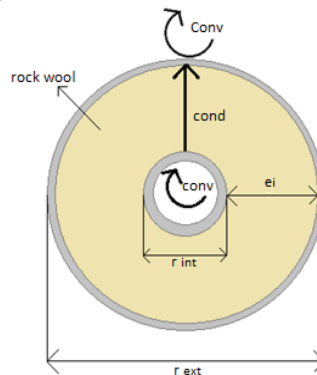


**FIGURE 2.** Heat transfer modes occurring for piping heat losses.

The insulation will be composed of rockwool ( $e_i$ ) with a thermal conductivity that has been assumed to be  $k_i = 0.06 \text{ W}\cdot\text{m}^{-1}\cdot\text{K}^{-1}$  [3] (value obtained for the average operating temperature). The Dittus-Boelter equation has been

used to estimate the Nusselt number and therefore the convection heat transfer coefficient between the HTF and the piping [4]:

$$Nu = 0.023 \cdot Re^{0.8} \cdot Pr^n, \\ Re > 10\,000 ; 0.7 < Pr < 160. \quad (1)$$

Conduction resistance through insulation has been assessed with a regular equation for a hollow cylinder, considering an internal radius of  $r_{int} = 0.044$  m and an exterior radius of  $r_{ext} = 0.194$  m.

The convective resistance between exterior insulation and the air has been assessed with the empirical relation described by Hilpert [5] and referenced in [6]:

$$Nu_D = c \cdot Re_D^m \cdot Pr^{1/3}, \quad (2)$$

where the constants  $c$  and  $m$  for the Reynolds number used are 0.027 and 0.805, respectively, and with all properties evaluated at the air film temperature,  $T_{air}$ . The air film temperature is the temperature of the air that is very close to the exterior insulation. In the present case, since the piping is well insulated, it has been assumed to be ambient temperature, i.e. 20 °C [7]. In addition, an average wind speed of 3.34 m.s<sup>-1</sup> was considered, which is obtained from an average of local meteorological data for Évora. According to the mentioned properties, the value obtained for the heat transfer coefficient is 15.2 W.m<sup>-2</sup>.K<sup>-1</sup>. Using this coefficient, the pipe section and its length, it was possible to obtain the value  $R_{conv}^{i-a}$ , in the different zones of the solar field. The total thermal resistance in the piping is then given by:

$$R_{eq}^{pipe} = R_{conv}^{f-p} + R_{cond}^i + R_{conv}^{i-a}, \quad (3)$$

A total heat loss from piping of about ~19 kW has therefore been calculated. Considering a total piping length of 207.6 m, the average value of the thermal losses per meter of piping (or linear heat losses) is:

$$P_{th,l}^{pipe} = \frac{P_{th}^{pipe}}{L_{tot}} = \frac{18987}{207.6} \approx 91.5 \text{ [W.m}^{-1}\text{]}. \quad (4)$$

**TABLE 1.** Results of the thermal losses obtained in the interconnecting piping.

Zone	Length [m]	$R_{eq}$ [K.W <sup>-1</sup> ]	$P_{th}^{pipe}$ [W]
1	52.3	0.075909	6323
2	24.7	0.16073	2986
3	20	0.198609	1359
4	81.8	0.04856	5560
5	28.8	0.137818	2757
<b>Total heat loss (W)</b>			<b>18987</b>

### Thermal Losses in the Solar Field

The linear heat loss values, with respect to the absorber tube temperature, are given by the receiver manufacturer. From the manufacturer data, a polynomial relation between linear heat losses and the fluid temperature was obtained. Since the losses are directly related to the ambient temperature, the correlation was obtained considering a  $\Delta T$  between the fluid temperature and an ambient temperature of 20 °C. This correlation is given by the following expression:

$$P_{th,l}^{receiver} \approx (1.912 \cdot 10^{-8}) \cdot (\Delta T_{r \rightarrow a})^4 - (1.336 \cdot 10^{-5}) \cdot (\Delta T_{r \rightarrow a})^3 + (4.088 \cdot 10^{-3}) \cdot (\Delta T_{r \rightarrow a})^2 - 0.0467 \cdot (\Delta T_{r \rightarrow a}) \text{ [W.m}^{-1}\text{]}. \quad (5)$$

Knowing that the inlet temperature in the solar field is 290 °C and the outlet temperature is 500 °C, a mean value of 250.5 W.m<sup>-1</sup> is obtained. Additionally, knowing that the solar field has a total length of 684 m it is possible to obtain the mean value of thermal losses in the receiver tubes.

$$P_{th}^{receiver} = P_{th,l}^{receiver} \cdot L = 250.5 \text{ (W.m}^{-1}\text{)} \cdot 684 \text{ (m)} \approx 171.5 \text{ [kW]}. \quad (6)$$

## Total Thermal Losses

Considering all the calculations made and taking the values of thermal losses obtained in the piping during the nominal operation of the platform, the total losses can be obtained:

$$P_{th}^{total} = P_{th}^{pipes} + P_{th}^{receivers} \approx 190.4 \text{ [kW]}. \quad (7)$$

In fact, linear thermal losses in the receiver tubes are 2.7 times greater than the linear thermal losses in interconnecting piping. Since the receivers are 3.3 times longer than the pipes, thermal losses in the receivers are approximately 9 times higher; representing about 90% of the total losses.

In addition, the total amount of thermal losses that are occurring in the interconnecting piping and receiver tubes during nominal operation accounts approximately for 5% of the solar field's nominal power.

## Night Thermal Losses

During night and cloudy periods, heat losses could lead to salt solidification. To tackle this issue it is possible to use electrical heat tracing to maintain the tubes at a safety temperature and/or using heat stored in the cold tank by circulating the salts in the solar field at a very low flow rate. In principle, the second option will be preferred as no extra electrical consumption will be required. However, it will reduce the net heat production of the plant. Thus, to understand the capacity of the cold tank to maintain the platform's piping and receivers heated at night, thermal capacity of the tank and thermal losses in the piping and receivers during the night must be calculated. From these values it is possible to determine how many hours heat stored in the cold tank can maintain the piping and receivers heated without running the risk of freezing.

### Tanks Thermal Losses

To determine thermal losses from the tank that will be used for this evaluation and as an input for SAM simulation, only the losses on the sides and tops of the tanks will be determined; the bottom losses are considered negligible. Insulation of the tanks is made through the use of rockwool similarly to the piping ( $k_i = 0.06 \text{ W}\cdot\text{m}^{-1}\cdot\text{K}^{-1}$ ). The tanks have the following presentation:

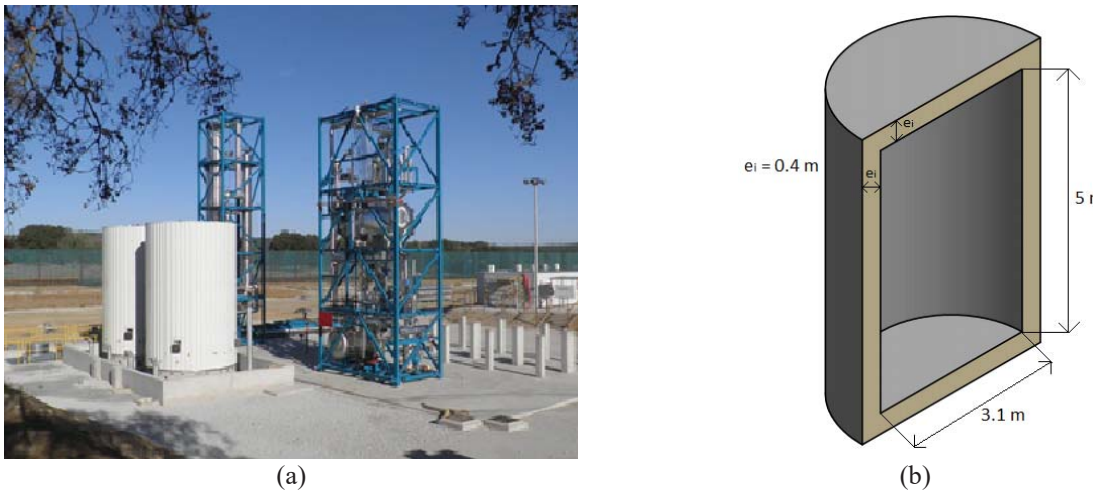


**FIGURE 3.** Scheme of the storage tanks: (a) Photograph of the actual storage tanks; (b) schematic diagram used for the calculations.

To calculate heat losses, the following assumptions are made: 1) the wall of the tank is at fluid temperature; 2) the ullage space is not considered, i.e. the tank is considered to be full of fluid. Thus, the estimated heat losses are overestimated. Moreover, two mechanisms for heat loss, at the tanks side and the top, are considered: 1) conduction through the tank's insulation; 2) tank's insulation and air convection. However, since they do not take into account

thermal bridges (through the structure, sensors, etc.), these assumptions may compensate each other and lead to an overall correct final estimation. The following information is considered:

**TABLE 2.** The main information about the tanks.

<b>Tanks characteristics</b>	
$r_{in}$ [m]	1.55
$r_{ext}$ [m]	1.95
$H_{tank}$ [m]	5
$e_i$ [m]	0.4
$k_i$ [W.m <sup>-1</sup> .K <sup>-1</sup> ]	0.06

Conduction resistance through side insulation is assessed with the regular equation for a hollow cylinder while resistance from the top is assessed with the regular equation for a defined thickness.

To determine the convective resistance between the tank's walls and air, it is necessary to consider the values presented in **TABLE 2**, as well as, air properties, available in [7]. The heat transfer coefficient between the walls of the tanks and air is calculated with the Zhukauskas relation (for Reynolds number  $2 \times 10^5 < Re < 2 \times 10^6$  and Prandtl number  $0.7 < Pr < 500$ ) [6]:

$$Nu = c \cdot Re^m \cdot Pr^n. \quad (8)$$

Where the correlation constants  $c$ ,  $m$  and  $n$  are 0.076, 0.700 and 0.370, respectively. With these values it is then possible to determine the equivalent thermal resistance of the tanks, knowing that the conductive and convective resistances at the side,  $R_{cond}^{t,side}$  and  $R_{conv}^{t,side}$ , respectively, and at the top of the tank,  $R_{cond}^{t,top}$  and  $R_{conv}^{t,top}$ , respectively, are in series with each other, and the side of the tank is in parallel with the top of the tank:

$$R_{eq}^{tank} = \left( \frac{1}{R_{cond}^{t,side} + R_{conv}^{t,side}} + \frac{1}{R_{cond}^{t,top} + R_{conv}^{t,top}} \right)^{-1} \approx 0.109228 \text{ [K} \cdot \text{W}^{-1}\text{]}. \quad (9)$$

Finally, considering ambient air temperature of 10 °C (night temperature), hot tank temperature to be 500 °C and cold tank temperature 290 °C, a total value of 7.1 kW for thermal losses from the tanks is obtained (please, see **TABLE 3**).

**TABLE 3.** Values of thermal losses from the tanks.

<b>Thermal losses of the tanks</b>	
	$P_{th}^{tanks}$ [kW]
Hot Tank	4.5
Cold Tank	2.6
<b>Total</b>	<b>7.1</b>

Using **TABLE 3** values, total thermal loss coefficient of the tanks ( $h_{storage}$ ) can be obtained by:

$$P_{th}^{tanks} = h_{storage} \cdot S \cdot \Delta T. \quad (10)$$

Where  $S$  corresponds to the total heat transfer surface and  $\Delta T$  the temperature difference between the tank and air. The value obtained through this equation is 0.163 W.m<sup>-2</sup>.K<sup>-1</sup> and this is the value entered in the software to perform the simulations.

### *Piping Thermal Losses*

To calculate the pipe thermal losses during night, it is important to consider the fluid's path during this period, please, see **FIGURE 4**.

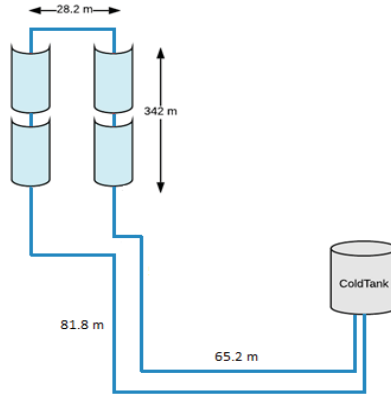


**FIGURE 4.** Trajectory of fluid during the night.

The resistances can be calculated knowing the information presented above, namely inner and outer radius of the pipe, insulation thickness and conductivity. In addition, considering a piping length of 175.2 m (corresponding to the night course).

For this calculation, the same method for thermal losses calculations during nominal operation is used. However, considering an ambient temperature of 10 °C, using the properties of HTF at 290 °C and knowing that during night the fluid will circulate at a very low mass flow rate of  $\sim 1 \text{ kg}\cdot\text{s}^{-1}$ .

Through the sum of conduction and convection resistances, the equivalent resistance value is obtained:  $R_{eq} = 0.022783 \text{ [K} \cdot \text{W}^{-1}]$ . Knowing the value of the equivalent resistance and using the following equation, the thermal losses are obtained:  $P_{th}^{pipes} = \Delta T / R_{eq} \cong 12290 \text{ [W]}$ . The thermal loss value during the night in the interconnecting piping is therefore  $\sim 12.3 \text{ kW}$ .

#### *Thermal Losses in Receiver Tubes*

Using **EQUATION 5** and considering that the average ambient temperature at night is 10 °C and that the receiver tube is at 290 °C, the following value of linear thermal losses in the receiver tube at night is obtained:  $P_{th}^{receivers} = 131.7 \text{ [W} \cdot \text{m}^{-1}]$ . Considering that the receiver tube has a total length of 684 m then the value of the thermal losses at night in the receiver tubes is:  $P_{th}^{receivers} = 131.7 \cdot 684.0 = 90060.0 \text{ [W]} \approx 90 \text{ [kW]}$ .

#### *Total Thermal Losses at Night*

Adding the losses in the interconnecting piping with the losses in the receiver tubes and in the tanks, the total heat loss value is:

$$P_{th}^{total} = P_{th}^{pipes} + P_{th}^{receivers} + P_{th}^{tanks} \approx 109399.5 \text{ [W]} \approx 109.4 \text{ [kW]}. \quad (11)$$

It should be noted that in this calculation, losses through pipe supports were not included; it was assumed that supports are well thermally insulated and, in this way, losses in these points can be neglected. To avoid severe heat losses in the pipe supports, that can lead to local salt freezing, these supports must be pre-insulated with, for example, calcium silicate rods, as calcium silicate offers the necessary thermal and mechanical resistances, despite being expensive. A low-cost concept for pre-insulated calcium silicate rods was recently presented [8].

#### *Thermal Inertia Capacity of the Cold Tank*

The thermal inertia capacity of the cold tank is the energy that can be lost by the system before reaching a minimum safety temperature that has been defined. When the salt is circulated, it is considered that its temperature will decrease in a homogeneous way in the whole plant. To determine the available energy in the tank, the following information must be considered:

**TABLE 4.** Important information to determine the capacity of the tank.

<b>Tank's characteristics</b>	
Tank Volume [m <sup>3</sup> ]	29
Density of the Hitec XL molten salt at 290 °C <sup>1</sup> [kg.m <sup>-3</sup> ]	2000
Specific heat of the Hitec XL molten salt at 290 °C [J.kg <sup>-1</sup> .K <sup>-1</sup> ]	1450
Minimum safety temperature <sup>2</sup> [°C]	200

<sup>1</sup>Initial temperature at which the cold tank is.

<sup>2</sup>To ensure that the temperature of the salt does not approach its freezing temperature.

Thermal inertia capacity of the cold tank is given by:

$$E_{th}^{tank} = V_{tank} \cdot \rho \cdot Cp \cdot \Delta T. \quad (12)$$

From this expression, where  $\Delta T$  is the value between the initial temperature of the cold tank (290 °C) and the minimum set safety temperature (200 °C), and the given values, it is possible to calculate thermal inertia capacity of the cold tank:  $E_{th}^{tank} \approx 2.10$  [MWh]. This value, along with the assessed thermal losses during night, allows estimation how many hours the cold tank can be used to maintain the salts above the minimum allowed temperature (see below).

### Operation Strategies for Night Period

The main problem of using MS as HTF in CSP plants is their high melting point. Thus, operating strategies of this type of plants are largely directed in maintaining salts at temperatures above safety temperature (in the literature it is defined as 30 °C above freezing point [9], but in this project it is set to 200 °C [1]), spending as little electricity as possible in this process. In this sense, there are numerous strategies that can be defined, as is the case of circulating the MS from the cold tank through solar field piping during night and cloudy periods. Knowing that total night heat losses are 109.4 kW and that the thermal inertia capacity of the cold tank between 290 °C and 200 °C is 2.1 MWh, it is expected that the latter will be able to maintain the system heated during about 21.2 hours, without solar irradiation. A more accurate estimation can be made by accounting for the fact that the total system heat loss decreases as the fluid temperature decreases.

To extend the period that the cold tank can maintain the piping heated without using electricity there are several strategies that can be defined, for example reducing the minimum temperature of the tank to increase its thermal inertia capacity. In the present case, it can be reduced to 170 °C and the number of hours that the cold tank can withstand will increase to 28.3 hours. This strategy reduces the necessity to use impedance heating in the receiver tubes and electrical heat tracing in the piping and thus reduce electricity consumption.

Another possibility is to leave some energy stored in the hot tank and to use this energy to heat the cold tank when the temperature of the latter is too low. In addition, in the periods of the year with less solar irradiation, a strategy that can be considered is to store the small amount of thermal energy that is obtained from the solar field at sunny occasions, instead of sending the heat to the steam generator; for later to be used to maintain the system heated and to avoid long periods of electricity consumption.

### SIMULATION WITH THE SYSTEM ADVISOR MODEL

The System Advisor Model (SAM) was developed by NREL in order to model a range of renewable energy including solar thermal parabolic troughs [10]. SAM uses an hourly performance model to estimate a power system's total annual output. The weather data file for this work was obtained through the meteorological station of the Institute of Earth Sciences in Évora, Portugal (N38.567686, W7.91172), being a reference station for the region. The meteorological data that were used are the result of a compilation between years 2016, 2017 and 2018.



## Annual Production of Energy and Capacity Factor

In the simulation model that is used, “Process heat parabolic trough”, the annual production of energy represents the amount of thermal energy that the plant produces during a year and the value is given in  $MWh_{th}$ . The capacity factor is a comparative measure of the amount of energy produced by a plant with the maximum energy that could be produced if the plant was operating at nominal power during the same period. In this case, considering the nominal steam generator power to be  $\sim 1.8$  MW, the capacity factor is obtained by the following equation:

$$CF = \frac{\text{Annual Energy Produced}}{(1.8 \times 10^6) \cdot 8760 \text{ hours}} \quad (13)$$

Through this value, it is possible to determine how much equivalent hours the plant is producing at nominal power during that year. Using the meteorological data of Évora and HPS2 project information, the simulation of platform’s operation gives the following values: annual production of thermal energy; capacity factor, corresponding number of hours at nominal power production. These are listed in **TABLE 5**.

**TABLE 5.** Results obtained through the simulation in SAM.

Simulation results	
Annual energy [ $MWh_{th}$ ]	4540
Capacity Factor	0.288
Hours	2522

The capacity factor of this installation is lower than the typical value of this type of plants because its solar multiple, that is to say the solar field oversizing (nominal power) with respect to the steam generator needs, is relatively high (it is 2.4 whereas typically it is 1.8) and because its storage capacity is very small (2 hours instead of 7.5 hours in many commercial plants).

## Annual Thermal Power Freeze Protection

Annual thermal power freeze protection is one of the values provided in the SAM summary table. It represents the thermal energy required to heat the storage system as well as the solar field, always ensuring the safety temperature range of the HTF. In this way, the amount of thermal energy required to heat the plant is presented in **TABLE 6**.

**TABLE 6.** Thermal energy needed to heat the storage system and the solar field.

Thermal energy needs for heating	
TES freeze protection [ $MWh_{th}$ ]	9.104
Solar field freeze protection [ $MWh_{th}$ ]	18.655
Annual total freeze protection [ $MWh_{th}$ ]	27.759

From **TABLE 6** it can be seen that it takes twice as much thermal energy to heat the solar field than to heat the tanks. This result was already predictable since most of the platform’s total thermal losses occur in the solar field, particularly in the receiver tubes. Observing the annual value of energy required for freeze protection, this corresponds to  $\sim 0.6\%$  of the annual production of the platform.

## Annual Electricity Consumption

In the annual electricity consumption determined by SAM simulations the electric energy spent is included, that is required to: 1) circulate the HTF along the solar field; 2) circulate fluid into the steam generator; 3) collector daily tracking; 4) TES freeze protection. The value found is to be: **annual electricity load  $\approx 31.446$  [ $MWh_e$ ]**. However, in order to have a better perception of the difference in the electricity spent with the pump system, an infinite thermal resistance was assumed in the tanks in order to remove the TES freeze protection from the electricity consumption.

The obtained value is: **annual electricity load  $\approx 22.342$  [MWh<sub>e</sub>]**. The energy spent in daily solar tracking is almost insignificant; this implies that the electricity spent to pump the fluid into the heat sink and solar field are the main components contributing to the overall electricity consumption. Such fact was not observed by pioneers in this subject [11]. For a better perception of these consumptions, the following graph show the energy spent to collectors tracking, to pump the HTF along the solar field and through the heat sink.

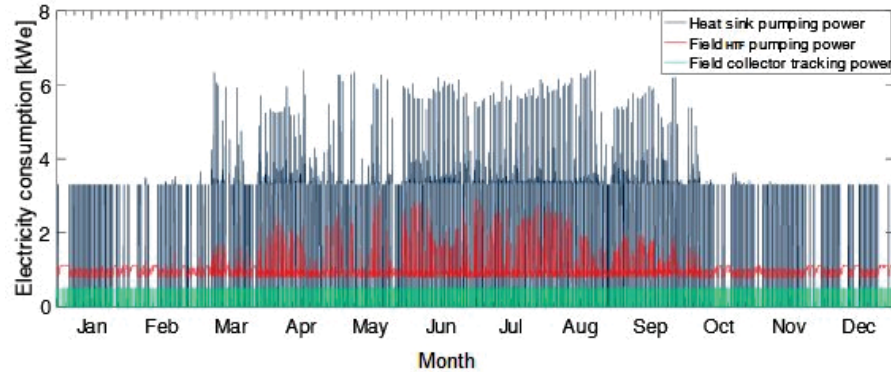


**FIGURE 5.** Annual electricity consumption on pumps and tracking.

However, as solar field heating will be done by impedance and electrical heat tracing, i.e., using electricity, it is important to account for the annual thermal power freeze protection at this point. For this, it is considered that the electrical resistances have an efficiency of 99% and total values of annual electricity consumption are shown in **TABLE 7**:

**TABLE 7.** Annual electricity consumption counting with solar field heating.

<b>Annual electricity consumption</b>	
Annual electricity load [MWh <sub>e</sub> ]	31.446
Annual electricity consumption for solar field freeze protection [MWh <sub>e</sub> ] <sup>1</sup>	18.843
Total annual electricity load [MWh <sub>e</sub> ]	50.289

The following figures allow to analyse in more detail the needs for solar field heating according to the time of year.

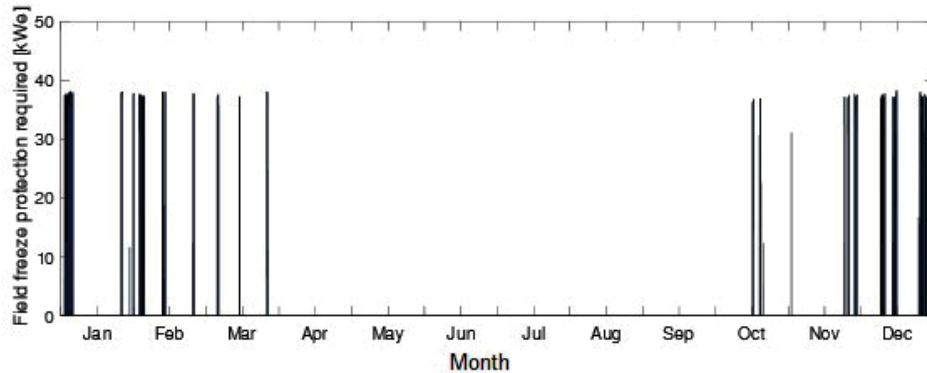


**FIGURE 6.** Annual field freeze protection required for HPS2 project.

<sup>1</sup> Value obtained through the SAM, where it is called “Annual thermal power for field freeze protection”.

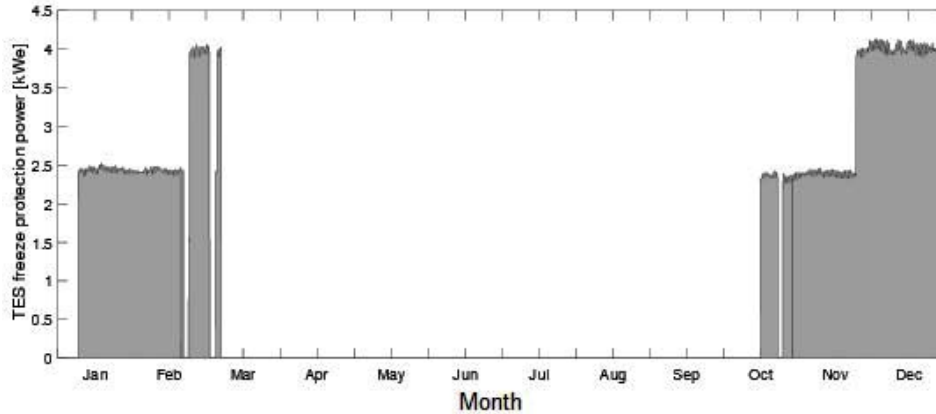


FIGURE 7. Annual TES freeze protection required for HPS2 project.

As can be seen from the image above, heating is only necessary for some periods of the coldest (and darkest) months of the year. For the rest of the year the thermal inertia of the fluid inside the pipes is sufficient to prevent the fluid from cooling to temperatures below the set safety temperature. However, this is the worst-case scenario. No operation strategy, as for example the circulation of salts from the cold tank through the piping during the night, is considered. And this latter strategy can significantly reduce the amount of electricity spent on solar field heating.

### Electricity Costs Estimate

Considering annual consumptions and that electricity has an estimated cost of 0.192 €/kWh, an estimate of annual electricity costs can be made: **annual electricity costs ≈ 9656 [€]**. Looking at the simulation results, of the 9656 € spent, 3618 € is for heating. This means that about 37% of annual electricity consumption is for HTF heating. However, using the strategies mentioned above this value will be lower. Thinking on a commercial scale, as the capacity of the tanks is higher as well as the amount of insulated piping, the thermal inertia capacity of both the tank and the piping will maintain the HTF heated for a longer period. Another important aspect is that when the amount of solar radiation reaching the collectors is low, SAM prioritizes production. In the case of HPS2, as no electricity is generated, the energy collected in the solar field can be all stored for later use in heating avoiding the highest consumption in the months of lowest radiation.

Finally, a brief remark is made here to say that the CAPEX value for MS despite the extra costs associated with the anti-freezing protection system (electrical heat tracing, impedance heating and pre-insulated piping supports), is expected to still be lower than the one for a commercial thermal-oil plant. This results from the savings in not buying thermal-oil (more expensive than the MS), nor heat exchanger (since the same HTF is used in the solar field as well as in the storage system), smaller storage tanks and less MS quantity (due to the higher operating temperature lower amount of MS is required and consequently smaller tanks) and only one group of pumps (there is only one working fluid and thus a single system pump, plus a back-up one, is required) are needed. A throughout comparison between solar power plant dependence of the levelized cost of electricity, LCOE, with the HTF used is made elsewhere [12].

### CONCLUSIONS

The purpose of HPS2 project is demonstrating the viability of using low-melting salts as heat transfer fluid in parabolic trough power plants. In addition to testing the viability and detecting possible problems that may arise, this project also aims to test operating strategies to reduce operational costs and make this type of plant as competitive as possible in terms of energy production costs. An example of these strategies is the circulation of salts stored in the cold tank through the solar field at night and cloudy periods. This reduces the need to use electrical resistances for anti-freezing protection, reducing the platform's electrical consumption. However, from this study it can be seen that high consumption is not expected with the salt under study, € 9656 per year, without any operating strategy. These results are due to the fact that YaraMOST is molten salt with an especially a low melting point. The scenario of a high melting point molten salt, such as Solar Salt, would be very different since the need for heating would be much higher and is subject to future analysis.

## ACKNOWLEDGMENTS

The HPS2 consortium acknowledges and highly appreciates the German Federal Ministry of Economic Affairs and Energy as well as the Projektträger Jülich for accompanying, supporting and generously funding the finalization of the molten salt demonstration plant (grant agreement number 0324097 and 0324018). HGS is grateful for the discussions held with Michael Wittman (HPS2 coordinator, DLR) and to Francis Lopes (University of Évora) for providing the meteorological data used in the simulations and to Mark Schmitz (TSK Flagsol) for a throughout revision of the manuscript.

## REFERENCES

1. M. Wittmann, M. Schmitz, H.G. Silva, P. Schmidt, G. Doppelbauer, J. Pancar, P. Santamaria, T. Miltkau, D. Golovca, L. Pacheco, D. Hogemann, M. Meyer-Grunefeldt, B. Seubert, "HPS2 - Demonstration of Molten-Salt in Parabolic Trough Plants - Design of Plant", *AIP Conference Proceedings*, 2126, 120024, 2019. DOI: 10.1063/1.5117642.
2. Rockwool, "The thickness of ROCKWOOL insulation," Rockwool specifications, 2009. [Online]. Available: [https://www.pipelagging.com/pdf/rockwool/Rockwool\\_Thickness\\_Guide.pdf](https://www.pipelagging.com/pdf/rockwool/Rockwool_Thickness_Guide.pdf)
3. A. A. Abdou e I. M. Budaiwi, "Comparison of Thermal Conductivity Measurements of Building Insulation Materials under Various Operating Temperatures," *Journal of Building Physics*, 29, pp. 171-184, 2005. DOI: 10.1177/1744259105056291.
4. I. Tosun, "Modeling in Transport Phenomena - A Conceptual Approach (Second Edition)", *Elsevier Science*, 2007.
5. R. Hilpert, "Heat Transfer from Cylinders," *Forsch. Geb. Ingenieurwes*, pp. 4-215, 1933.
6. S. Kaseb and G. El-Hariry, "Forced Convection Correlations," *Cairo University - Faculty of engineering*, 2006. [Online]. Available: <http://www.pathways.cu.edu.eg/ec/text-pdf/part%20b-9.pdf>
7. Y. S. Touloukian, P. E. Liley and S. C. Saxena, "Thermophysical Properties of Matter," in *Vol. 3: Thermal Conductivity*, vol. 3, 1970.
8. G.C. Delgado, P.R. Martins, H.G. Silva, "HPS-2 - Design of Pre-insulated Pipe Supports for Molten-Salt Technologies, K. Schmitz", Poster presentation, *SolarPACES 2019*, 1-4 October 2019, Daegu, South Korea.
9. A. Bonk, S. Sau, N. Uranga, M. Hernaiz e T. Bauer, "Advanced heat transfer fluids for direct molten salt line-focusing CSP plants," *Progress in Energy and Combustion Science*, pp. 69-87, 2018. DOI: 10.1016/j.pecs.2018.02.002.
10. NREL, "System Advisor Model (SAM)", 2010. [Online]. Available: <https://sam.nrel.gov/>
11. D. Kearney, U. Herrmann, P. Nava, B. Kelly, R. Mahoney, J. Pacheco, R. Cable, N. Potrovitz, D. Blake e H. Price, "Assessment of a Molten Salt Heat Transfer Fluid in a Parabolic Trough Solar Field," *J. Sol. Energy Eng.*, pp. 170-176, 2003. DOI: 10.1115/1.1565087.
12. T. Lopes, T. Fasquelle, H.G. Silva, "Pressure drops, heat transfer coefficient, cost and power block structure for a direct storage parabolic trough power plant running molten salts", *Solar Energy Materials and Solar Cells*, submitted (2020).